Available online at www.sciencedirect.com

ScienceDirect

Procedia CIRP 107 (2022) 984–990

www.elsevier.com/locate/procedia

55th CIRP Conference on Manufacturing Systems

Modeling of the Lithium Calendering Process for Direct Contact Prelithiation of Lithium-Ion Batteries

Benedikt Stumper[a]*, Jonas Dhom[a], Lukas Schlosser[a], David Schreiner[a], Andreas Mayr[a], Rüdiger Daub[a]

[a]*Institute for Machine Tools and Industrial Management, Technical University of Munich, Bolzmanstr. 15, 85748 Garching, Germany*

* Corresponding author. Tel.: +49-89-289-15539; fax: +49-89-289-15555. *E-mail address:* benedikt.stumper@iwb.tum.de

Abstract

The automotive industry's rapid advancement and complex demands concerning energy storage capacities and service life require lithium-ion batteries with improved energy density and cycle life. There are several ways to improve these two performance indicators for battery cells, such as using innovative, high-capacity electrode materials or novel and improved processes within battery production. One approach is prelithiation, a method to compensate for the initial capacity losses occurring either during the cell formation or during battery operation through the addition of lithium during cell production. In the case of direct contact prelithiation, thin lithium foils with a thickness below 10 µm are necessary to ensure the safe and accurate execution of the prelithiation process. However, the commercial availability of free-standing lithium foils is limited to minimum thicknesses of down to only 20 µm. For this reason, the present work examines in detail the calendering process of lithium. As part of a comprehensive parameter study, the influences of lithium foil geometries, line load, and roller temperature on the deformation behavior of lithium during calendering are investigated. A suitable process model is developed to understand the processing and thickness reduction of lithium and the calendering of lithium foils for direct contact prelithiation. For this purpose, a model based on empirical and semi-analytical approaches using fundamental physical interactions during calendering and material properties is developed and is parameterized based on experimental investigations on a laboratory scale. The combination of empirical and analytical modeling allows predictions about lithium processing and their validity ranges. The modeling intends to enable upscaling of the process and a transferability of direct contact prelithiation to the production of lithium-ion batteries on an industrial scale. Finally, the developed model contributes to understanding metallic lithium processing and its use for direct contact prelithiation in a roll-to-roll process and enables transferability of direct contact prelithiation to the production of lithium-ion batteries.

Keywords: lithium-ion batteries; prelithiation; lithium metal; calendering; process modeling;

1. Introduction

The present shift within the transportation sector, from combustion engines and fossil fuels to electric vehicles (EVs) and zero-emission mobility, challenges today's battery industry. Lithium-ion batteries (LIBs) as electrochemical energy storage systems are crucial for EVs to reduce CO_2 and NO_x emissions. However, to increase the market share of EVs, the LIB has further challenges to overcome and requires additional improvements in terms of energy density, cycle life, safety, and cost reduction [1, 2].

Today's LIBs suffer from initial capacity losses evoked by the formation of the solid electrolyte interphase (SEI) and from cyclic losses during cell operation due to further reactions within the battery cell. These reactions strongly depend on the electrode material used and "consume" lithium-ions, which are responsible for the charge transfer and thus for the energy provision of the battery cell. Therefore, the loss of lithium-ions reduces the energy density and the cycle life. [3]

2212-8271
10.1016/j.procir.2022.05.096

Prelithiation is an approved approach on a laboratory scale to compensate for the loss of lithium-ions as charge carriers. It can be defined as a pretreatment of electrodes whereby lithium is added to the cell before the first charge and discharge cycle of the formation process [4]. The main objective is to increase the energy density and the cycle life by compensating for both the lithium losses during formation and cell aging [4, 5]. To date, various prelithiation methods have already been investigated in the literature. A summary and description of these methods are given by Stumper et al. [6]. To date, none of these prelithiation approaches have been implemented on an industrial scale. Stumper et al. [6] investigated the design of a scalable roll-to-roll process for direct contact prelithiation using metallic lithium foil. Due to its flexible application, compatibility with common electrode materials, scalability, and cost-efficiency, direct contact prelithiation offers a promising method for industrial application [6]. The current state-of-the-art anodes require only small amounts of lithium and consequently very thin lithium foil thicknesses to ensure a safe and efficient process [6]. To obtain these thin foil thicknesses through the thinning of the lithium by calendering and, in the best case, directly applying it onto the electrode is crucial. However, to enable the calendering process for direct contact prelithiation using lithium foil and for the implementation within lithium-ion battery production, a profound process comprehension and understanding of the deformation behavior of lithium during calendering is necessary. Modeling approaches for the calendering process discussed in the literature focus on investigating the compaction properties of the electrodes [7–10] or on the calendering of dense material characterized by a homogeneous and solid cross microstructure with thicknesses of several millimeters [11]. To the best of our knowledge, the calendering of thin lithium foil with thicknesses below 100 µm has not yet been investigated.

The present work presents a model to describe the lithium calendering process. It consists of empirical and semi-analytical modeling approaches to systematically analyze the lithium calendering process and derive information necessary for a detailed process understanding. The model allows predictions about the geometric dimensions of the lithium foil after calendering and thus an accurate deployment of the calendering process for direct contact prelithiation.

2. Modeling of the lithium calendering process

2.1. Overall structure of the model

First, the structure of the model is presented, followed by a detailed description of its components. The main component of the overall process model is the combination of empirical and analytical modeling, as shown in Figure 1. The data are generated through a systematic design of experiments (DoE) and processed with the developed model. The focus within the empirical data is the information on the thickness reduction through calendering of the lithium. Further input variables are different process parameters, material characteristics, and geometry, influencing the foil thickness after calendering. The thickness of the lithium foil after calendering obtained from the empirical model is further processed with analytical approaches. The output variables of the process model are primarily used to increase the understanding of the process. A vital output variable is a change in foil geometry, which is of significant importance for the direct contact prelithiation of the electrode [6].

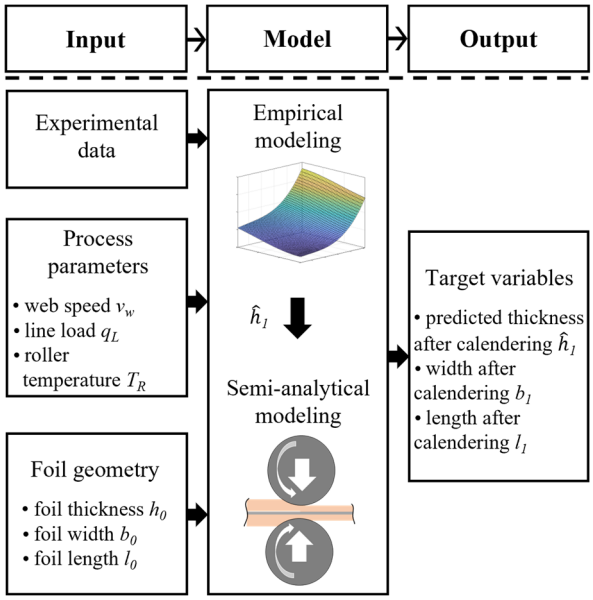

Figure 1. Schematic structure of the process model for the calendering of lithium foil.

2.2. Experimental setup and model assumptions

The experiments and investigations for the development, parameterization and validation of the model were carried out using a laboratory calender (GKL 300, SAUERESSIG Group, Germany) enclosed in a glovebox system (GS GLOVEBOX Systemtechnik GmbH, Germany) under argon atmosphere (O_2 < 0.5 ppm, H_2O < 0.5 ppm, temperature ~ 20 °C). Copper foils (SE-Cu/Cu-HCP, Schlenk Metallfolien GmbH & Co. KG, Germany) with thicknesses of 12 µm were used as carrier foils for all experiments. The lithium foil had a thickness of 50 µm and a purity of 99.9% (China Energy Lithium Co. LTD, China). The lithium samples used for the experiments each had a length and width of 18 mm ($b_0 = l_0$), respectively. A schematic illustration of the used sample setup is shown in Figure 2.

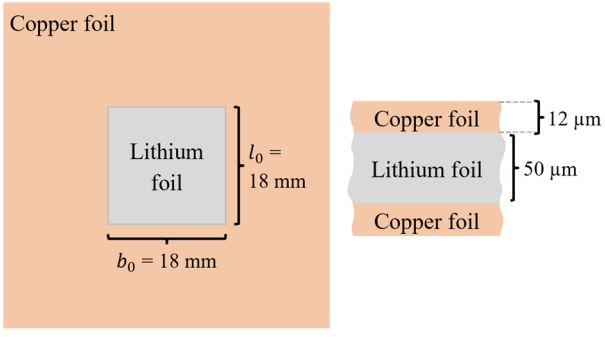

Figure 2. Schematic illustration of the sample setup for the conducted experiments. Top view (left) and cross-section (right) of the multi-layered sample setup consisting of lithium foil and copper foil as carrier foil.

The model developed within the scope of this work was implemented using MATLAB. For the development and construction of the model, various assumptions were made, which are listed below:

- The lithium is isotropic, which means that its deformation is independent of direction.
- The density of the lithium foil does not change before and after calendering; therefore, the volume constancy is valid [12].
- There is no relative sliding between the lithium foil and the carrier foil as well as between the calender roller and the rolled material. Friction effects are also neglected.
- The temperature distribution is uniform throughout the calendered material [13].
- For the copper carrier foil, it is assumed that due to the much larger Young's modulus compared to lithium ($E_{Cu} \gg E_{Li}$), no deformation of the copper occurs due to the line loads applied in the experiments [14, 15].

2.3. Empirical model

The empirical modeling aims to predict values for the thickness after calendering h_1 based on the evaluation of experimental investigations. The predicted values are expressed as $\widehat{h_1}$. The input data for this model are experimentally obtained, which are generated using a full factorial DoE. A range of values is defined for each input parameter, divided into values for parameterization and validation [16]. The value ranges are represented in the form of vectors, as shown in equation (1), exemplary for the factor line load q_L. Each component of the vector represents a parameter value, which is varied during the experimental investigation.

$$\vec{q}_L = [q_{L_1}, q_{L_2}, q_{L_3} q_{L_4}, q_{L_5}] \tag{1}$$

The vector for the input parameter of the roller temperature T_R is created accordingly. The web speed v_w and the input thickness of the lithium foil h_0 are kept constant within the scope of these investigations. Within the full factorial DoE, each value of one parameter vector is combined with each of the values of the other parameter vectors. If the determined values of h_1 are represented over the entire vector of $\vec{q}_L$ while keeping the values of T_R and h_0 constant, the term *two-dimensional factor space* is used since the target variable h_1 is the second dimension. Figure 3 illustrates the two-dimensional factor space showing the relationship between q_l and h_1.

Due to the non-linear and exponential relationship in Figure 3, a third-degree polynomial is used for the empirical modeling. The polynomial used has the form of equation (2) and respective coefficients k_n are determined by regression.

$$f(q_L) = k_1 {q_L}^3 + k_2 {q_L}^2 + k_3 q_L + k_4 = \widehat{h_1} \tag{2}$$

The empirical model allows predictions beyond the experimentally obtained values. However, this is only valid for values which are in this two-dimensional factor space (Figure 3) and for the investigated values of T_R and h_0.

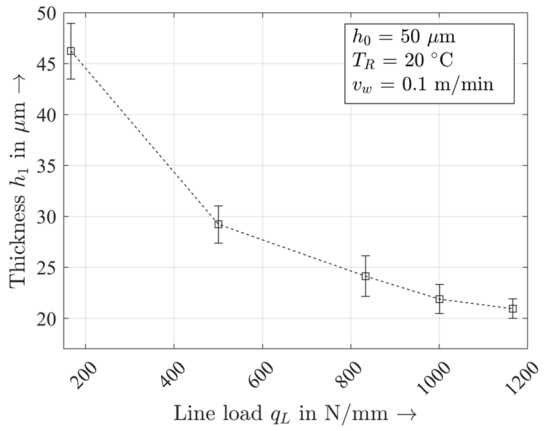

Figure 3. Representation of the two-dimensional factor space of the thickness h_1 over the line load q_l for h_0 = 50 µm, T_R = 20 °C, v_w = 0.1 m/min. The mean values and standard deviations refer to five measured values in each case.

The experimentally obtained data can be described in a three-dimensional factor space, represented by equation (3). This equation describes the assignment between q_L, T_R and h_1, where h_1 is a point in the three-dimensional factor space.

$$f(\vec{q}_L, \vec{T}_R)_{h_0, v_w = const.} = h_1 \tag{3}$$

To provide a prediction $\widehat{h_1}$ of the thickness after calendering depending on the process parameters used, the two-dimensional factor space is extended by a further dimension within the framework of the empirical modeling. This is done by linking the vector $\vec{q}_L$ with the vector $\vec{T}_R$. The values for $\vec{q}_L$ are calculated from the applied force (3, 6, 9, 12, 15, and 21 kN) of the calender and the width of the lithium foil (18 mm). The remaining input parameters h_0 and v_w remain constant. This results in a three-dimensional factor space which assigns a value of h_1 to each linkage of the components of the vectors $\vec{q}_L$ and $\vec{T}_R$ (see equation (3)). The vectors $\vec{T}_R$ and $\vec{q}_L$ as well as the parameters h_0 and v_w describe the considered three-dimensional factor space and are given hereafter.

- $\vec{T}_R$ = [20, 40, 60, 80] °C
- $\vec{q}_L$ = [167, 500, 833, 1000, 1167] N/mm
- h_0 = 50 µm
- v_w = 0.1 m/min

Figure 4 shows the three-dimensional factor space for the vectors and parameters described above. The red points represent the experimental data used for equation (3) for the model's parameterization. As already observed by Schreiner et al. [17] for battery cathodes, calendering of lithium foil also requires a lower line load for thickness reduction as the roller temperature increases. In addition, it can be observed that the relationship is not linear but exponential, meaning that the thinner the foil becomes, the more force must be applied for further thickness reduction.

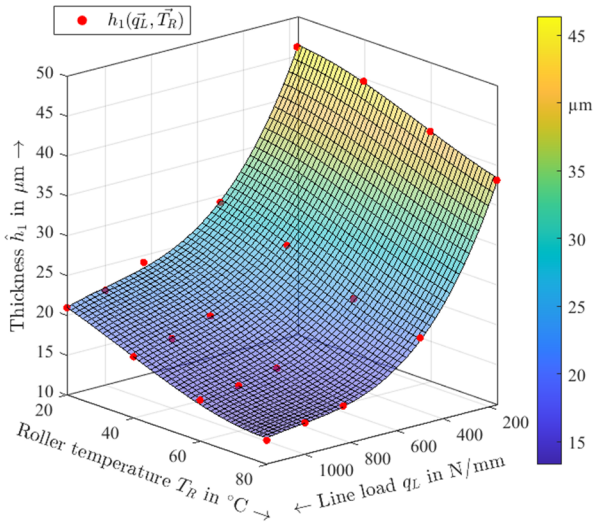

Figure 4. Representation of the empirical modeling for the three-dimensional factor space with h_0 = 50 µm, v_w = 0.1 m/min.

Using the parameterization values shown in red, a functional relationship can be determined using a multiple linear regression that provides a prediction $\widehat{h_1}$ for the thickness of the lithium after calendering as a function of the two input parameters T_R and q_L. In Figure 4, this functional relationship is represented by the color-graded plane, described by the equation (4).

$$f(q_L, T_R) = k_1 + k_2 q_L + k_3 T_R + k_4 {q_L}^2 + k_5 q_L T_R + k_6 {T_R}^2 + k_7 {q_L}^3 + k_8 {q_L}^2 T_R + k_9 q_L {T_R}^2 + k_{10} {T_R}^3 = \widehat{h_1} \quad (4)$$

The coefficients k_n are determined by linear regression. With these coefficients, a functional relationship is obtained, which fully predicts the relationships in the three-dimensional factor space.

The predicted thickness $\widehat{h_1}$ is used with the help of the extension of the empirical model by analytical approaches to predict the lithium's changes in width and length. This semi-analytical modeling is described in the following section.

2.4. Semi-analytical model

By combining empirical and semi-analytical modeling, it is possible to make predictions about the change in thickness and the changes in length and width of the lithium foil. Through analytical approaches, the geometric dimensions of the lithium foil resulting from calendering can be completely described.

For the semi-analytical modeling, it is assumed that the volume of the calendered material remains the same before and after calendering. Therefore, the constancy of the volume can be derived from the conservation of mass for constant density, which is expressed within equation (5), where V_0 describes the input volume and V_1 the output volume of the calendered lithium [11, 12, 18].

$$V_0 = V_1 \quad (5)$$

This equation can be converted for a cuboid with the input geometry h_0, b_0 and l_0 into the output geometry h_1, b_1 and l_1 (see equation (6)). Where h_0, b_0 and l_0 are the thickness, the width and the length of the lithium before calendering and h_1, b_1 and l_1 respectively after calendering.

$$h_0 \cdot b_0 \cdot l_0 = h_1 \cdot b_1 \cdot l_1 \quad (6)$$

Figure 5 shows a cross-sectional view of the calendering process (material flow from left to right) and illustrates the geometrical relationship between input and output geometry. The plane EE' is the entry plane and the plane AA' is the exit plane. Between the radius r_r to the entry and exit plane spans the roller angle α_0. The pressed length is represented by the formula symbol l_d and the angular velocity of the roller is represented by ω. The change in foil thickness due to calendering ($h_0 - h_1$) is described by Δh.

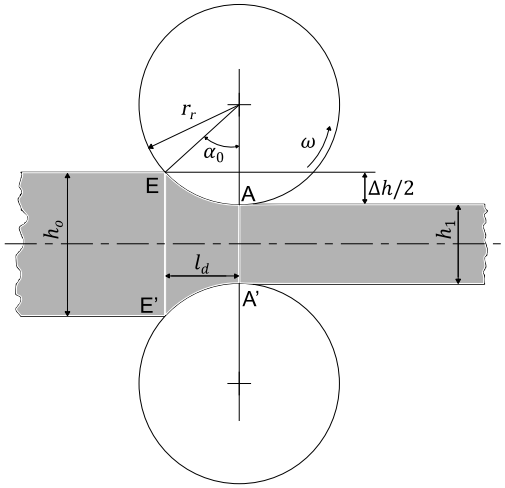

Figure 5. Cross-sectional view of a schematic calendering process and the geometrical relationships between the calendered material before and after calendering [11].

To calculate the width changes of the calendered object, there are several analytical equations that use different calculation approaches. The equation (7), according to *Riedel* [19], uses the geometric relations between the material before and after calendering to calculate the change in width Δb.

$$\Delta b = \frac{b_0 \cdot \Delta h \cdot l_d}{\sqrt{\frac{b_0}{l_d}} \cdot b_0 \cdot h_0 + h_1 \cdot l_d} \quad (7)$$

An alternative width equation, which considers the geometry of the roller gap in more detail and the radius of the calendering roller r_r is the equation (8) according to *Roux* [11].

$$\Delta b = \frac{\Delta h \cdot \left(\frac{b_0}{h_0}\right)}{(1 + 0.57 \cdot B) \cdot \left[1 - \frac{\Delta h}{h_0} + \frac{3 \cdot A}{\left(2 \cdot \frac{r_r}{h_0}\right)^{\frac{3}{4}}}\right]} \quad (8)$$

Within equation (8), A and B are constants that are calculated using equations (8) and (9).

$$B = \left(\frac{b_0}{h_0} - 1\right) \cdot \left(\frac{b_0}{h_0}\right)^{\frac{2}{3}} \tag{9}$$

$$A = \left(1 + 5 \cdot \left(0.35 - \frac{\Delta h}{h_0}\right)^2\right) \cdot \sqrt{\frac{h_0}{\Delta h} - 1} \tag{10}$$

The third width equation used in the presented model is the *Falk* [19] equation (11), which is based on the rolling angle α_1 at 100% thickness reduction.

$$\Delta b = \sqrt{\frac{0.161 \cdot \Delta h \cdot b_0 \cdot (h_0 + h_1)}{h_1 \cdot \alpha_1} + b_0^2} - b_0 \tag{11}$$

The three presented width equations are evaluated in section 4 regarding their accuracy and suitability for the process model, determining the choice of the correct equation.

In summary, the combination of the empirical and semi-analytical model allows determining output variables that provide information about the deformation of the lithium foil after calendering. With this information, the model also gives a detailed understanding of the interactions between the different variables and parameters of the calendering process.

3. Validation of the empirical model

For the validation of the model, the residuals r in the three-dimensional space are considered. These result from the deviation between the predicted values of the model $\widehat{h_1}$ and the values h_1 of the parameterization. Figure 6 illustrates the residuals, where the plotted plane with the values for the residuals of 0 symbolizes the parameterization data and the blue lines the respective residual between h_1 and $\widehat{h_1}$. Figure 6 shows that the deviations of the predicted values from the measured parametrization values are below ± 1.8 µm, which is represented by the lengths of the residuals (blue lines). For the largest residuum, this deviation is about 6.3% referred to the measured value.

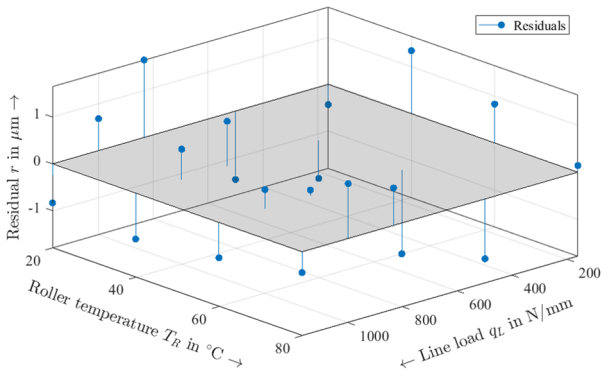

Figure 6. Illustration of the residuals between the predicted values and the parameterization values for the calculation of the coefficient of determination R^2.

These residuals in the three-dimensional space are included in the calculation of the coefficient of determination R^2 [20], which is an indicator for the quality of the regression [21] and is defined in equation (12).

$$R^2 = \frac{\sum_{i=1}^{20}\left(\hat{h}_{1_i} - \bar{h}_{1_i}\right)^2}{\sum_{i=1}^{20}\left(h_{1_i} - \bar{h}_{1_i}\right)^2} \tag{12}$$

The closer the calculated value is to 1, the higher the quality of the calculated regression [21]. For the present example, this R^2 value is 0.99, which indicates a high prediction quality for the model presented.

The determined regression equation (4) is then transferred to the different two-dimensional factor spaces by using one value for the roller temperature T_R (for T_R = 20, 40, 60, 80 °C) at a time. Specific confidence intervals can be described in the two-dimensional space using these regression equations. This procedure is illustrated in Figure 7. The validation data are then evaluated for their position within the confidence intervals of 95%. The empirical model is considered valid if the validation data are located within this confidence interval [21], which is the case for the presented regression. This validation procedure is repeated for all roller temperatures of the vector $\vec{T}_R$.

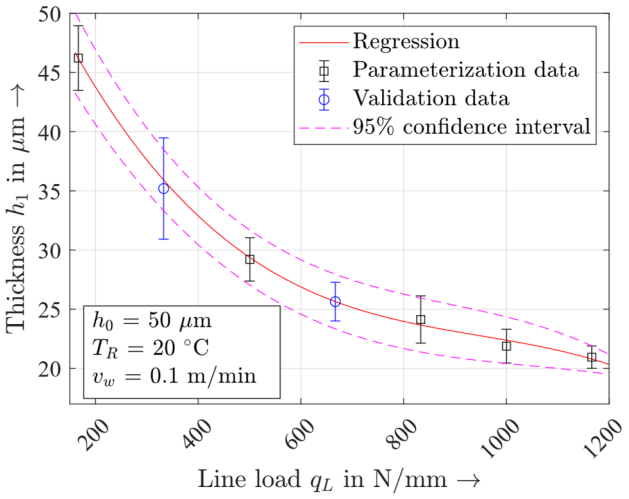

Figure 7. Validation of the calculated regression using the validation data set and confidence intervals of 95%. The mean values and standard deviations refer to five measured values in each case.

4. Parameterization of the semi-analytical model

To parameterize the semi-analytical model, experiments were conducted using the previously described experimental setup (see section 2.2). The lithium foil with a thickness of 50 µm is calendered with a line load of 1164 N/mm and a web speed of 0.1 m/min. The changes in width and length of the calendered lithium foil were measured with an accuracy of ± 0.1 mm. Within the parameterization of the semi-analytical model, the width equations according to *Riedel, Roux* and *Falk* (equations (7), (8) and (11)) are evaluated for their suitability for the model. For this purpose, the parameterization data from Table 1 are used.

Table 1. Comparison of experimental (left) and calculated (right) data. The values are generated by calendering lithium foils with a thickness of 50 µm with a line load of 1164 N/mm at T_R = 20 °C. The width and length of the processed lithium samples were 55 mm and 18 mm, respectively. The mean value for h_1 is 21.76 ± 0.14 µm, determined by five measurements.

Experimental data in mm	Calculated data in mm
	Riedel: $b_1 = 55.16$
$b_1 = 55.0$	*Roux*: $b_1 = 55.00$
	Falk: $b_1 = 55.00$
	Riedel: $l_1 = 41.23$
$l_1 = 41.8$	*Roux*: $l_1 = 41.35$
	Falk: l_1= 41.35

Based on the changes in width and length from Table 1, it can be concluded that all width equations are suitable for the semi-analytical model due to the minor deviations of the calculated data from the measured values. Since it is desirable to use a broad consideration of the geometry within this work, the *Roux* equation is selected for use in the presented model. Another reason for using the *Roux* equation is that it takes the calender roller radius into account, enabling the model's transferability to other calendering systems.

5. Discussion

The developed model, which was initially illustrated in Figure 1 and was implemented using MATLAB, aims to create a more profound process understanding of the calendering of lithium foil. The combination of empirical and semi-analytical modeling approaches provides valid statements about the process results of calendering lithium foil within the defined parameter spaces. The process output (deformed lithium foil) can be fully described by combining empirical and semi-analytical modeling. After parameterization, the model allows predictions about the resulting foil thicknesses and dimensional changes for a given initial foil thickness and given process parameters. This model can significantly reduce the experimental effort required to adjust the calendering process and provides a profound understanding of the process of lithium calendering and its use for direct contact prelithiation of battery electrodes.

Since individual foil pieces are sometimes necessary for this purpose due to the electrochemical requirements of the battery cell and the commercially available lithium foil thicknesses, it is essential to determine the deformation of the lithium pieces in all three spatial directions. It thus offers the possibility of adapting the lithium foil quantity precisely to the individually required degree of prelithiation for the electrode. In addition, the model provides the basis for its extension by additional process parameters and expanding the factor spaces considered. This enables the transferability to other calendering systems and thus the scalability of the process.

6. Conclusion

To enable direct contact prelithiation using lithium foil for lithium-ion battery production, thin lithium foil (< 10 µm) or foil pieces with precisely defined geometric dimensions are required. In both cases, an in-depth understanding of lithium foil calendering is essential to ensure a controlled deposition process as well as safe and efficient cell operation.

With the semi-analytical model presented in this paper, it is possible to predict how and to what extent thicker lithium foils can be calendered to lower thicknesses. Due to the ability to produce thinner lithium foils, the use of the presented model creates an economic benefit since lithium foil becomes more expensive as thickness decreases [22, 23].

The presented model for the calendering of lithium foil allows profound insights into the cause-effect relationships during the calendering of lithium. In addition, the model provides a better understanding of the deformation process, which can reduce the setting up of the experiments. This can reduce material consumption and shorten the time of the experiments to set up the process. By predicting the lithium foil's thickness, width, and length changes using the developed model, the calendering process can be enabled for the roll-to-roll application of lithium foil on battery electrodes in the context of direct-contact prelithiation in a commercial application. The information on the geometric changes can be used by applying continuous lithium foil and applying individual pieces of lithium foil.

The outcome of this work serves as a basis for further extending the parameter spaces of the model with the aid of experimental data from larger calendering systems and its transferability to larger scales, up to an industrially relevant scale-up of the process. Current investigations are also concerned with the influence of web speed on the calendering of lithium and the transferability to other foil geometries. Therefore, it is intended to extend the model to include the process parameter web speed, thus providing further information on the scalability of lithium foil calendering.

Acknowledgments

The presented work is part of the research project ‘SPIDER’ (Safe and Prelithiated hIgh energy DEnsity batteries based on sulphur Rocksalt and silicon chemistries). We express our gratitude to the European Union for funding the project under grant agreement number 814389. Furthermore, we would like to thank our research partners for their constructive work and support within the SPIDER project.

References

[1] Kwade, A., Haselrieder, W., Leithoff, R., Modlinger, A. *et al.*, 2018. Current status and challenges for automotive battery production technologies *3*, p. 290.

[2] Scrosati, B., Garche, J., 2010. Lithium batteries: Status, prospects and future *195*, p. 2419.

[3] Goodenough, J.B., Park, K.-S., 2013. The Li-ion rechargeable battery: a perspective. J Am Chem Soc *135*, p. 1167.

[4] Chevrier, V.L., Liu, L., Wohl, R., Chandrasoma, A. *et al.*, 2018. Design and Testing of Prelithiated Full Cells with High Silicon Content *165*, A1129-A1136.

[5] Holtstiege, F., Bärmann, P., Nölle, R., Winter, M. *et al.*, 2018. Pre-Lithiation Strategies for Rechargeable Energy Storage Technologies: Concepts, Promises and Challenges *4*, p. 4.

[6] Stumper, B., Mayr, A., Reinhart, G., 2020. Application of Thin Lithium Foil for Direct Contact Prelithiation of Anodes within Lithium-Ion Battery Production *93*, p. 156.
[7] Meyer, C., Kosfeld, M., Haselrieder, W., Kwade, A., 2018. Process modeling of the electrode calendering of lithium-ion batteries regarding variation of cathode active materials and mass loadings *18*, p. 371.
[8] Sangrós Giménez, C., Schilde, C., Froböse, L., Ivanov, S. *et al.*, 2020. Mechanical, Electrical, and Ionic Behavior of Lithium‐Ion Battery Electrodes via Discrete Element Method Simulations *8*, p. 1900180.
[9] Schreiner, D., Klinger, A., Reinhart, G., 2020. Modeling of the Calendering Process for Lithium-Ion Batteries with DEM Simulation *93*, p. 149.
[10] Schreiner, D., Lindenblatt, J., Günter, F.J., Reinhart, G., 2021. DEM Simulations of the Calendering Process: Parameterization of the Electrode Material of Lithium-Ion Batteries *104*, p. 91.
[11] Christian Overhagen, 2018. *Modelle zum Walzen von Flach- und Vollquerschnitten*, Essen.
[12] Orowan, E., 1943. The Calculation of Roll Pressure in Hot and Cold Flat Rolling *150*, p. 140.
[13] Sangrós, C., Schilde, C., Kwade, A., 2016. Effect of Microstructure on Thermal Conduction within Lithium-Ion Battery Electrodes using Discrete Element Method Simulations *4*, p. 1611.
[14] Buch, A., 1999. *Pure metals properties: A scientific-technical handbook*. ASM International; Freund Publishing House, Materials Park, Ohio, London.
[15] Tariq, S., Ammigan, K., Hurh, P., Schultz, R. *et al.*, 2003. LI material testing- fermilab antiproton source lithium collection lens, in *Proceedings of the 2003 Bipolar/BiCMOS Circuits and Technology Meeting (IEEE Cat. No.03CH37440)*, IEEE, p. 1452.
[16] Rebala, G., Ravi, A., Churiwala, S., 2019. *An Introduction to Machine Learning*. Springer, Cham.
[17] Schreiner, D., Oguntke, M., Günther, T., Reinhart, G., 2019. Modelling of the Calendering Process of NMC‐622 Cathodes in Battery Production Analyzing Machine/Material‐Process‐Structure Correlations *7*, p. 1900840.
[18] A new analyitcal model for cold Rolling of sheet and strip, 2011. *Gustavo Echave*.
[19] Werner Lueg, Editor. *Die Ermittlung der Breitenzunahme beim Warmwalzen von Stahl auf glatter Walzbahn: Archiv für das Eisenhüttenwesen*.
[20] Fahrmeir, L., Kneib, T., Lang, S., Marx, B., 2013. *Regression: Models, methods and applications*. Springer, Berlin, Heidelberg.
[21] Kleppmann, W., 2016. *Versuchsplanung: Produkte und Prozesse optimieren,* 9th edn. Hanser, München.
[22] Yan, J., Cao, W.J., Zheng, J.P., 2017. Constructing High Energy and Power Densities Li-Ion Capacitors Using Li Thin Film for Pre-Lithiation *164*, A2164-A2170.
[23] Schmuch, R., Wagner, R., Hörpel, G., Placke, T. *et al.*, 2018. Performance and cost of materials for lithium-based rechargeable automotive batteries *3*, p. 267.